M.R. Krishnamurthy, B.J. Gireesha*, B.C. Prasannakumara, and Rama Subba Reddy Gorla

Thermal radiation and chemical reaction effects on boundary layer slip flow and melting heat transfer of nanofluid induced by a nonlinear stretching sheet

DOI 10.1515/nleng-2016-0013
Received March 14, 2016; accepted July 21, 2016.

Abstract: A theoretically investigation has been performed to study the effects of thermal radiation and chemical reaction on MHD velocity slip boundary layer flow and melting heat transfer of nanofluid induced by a nonlinear stretching sheet. The Brownian motion and thermophoresis effects are incorporated in the present nanofluid model. A set of proper similarity variables is used to reduce the governing equations into a system of nonlinear ordinary differential equations. An efficient numerical method like Runge-Kutta-Fehlberg-45 order is used to solve the resultant equations for velocity, temperature and volume fraction of the nanoparticle. The effects of different flow parameters on flow fields are elucidated through graphs and tables. The present results have been compared with existing one for some limiting case and found excellent validation.

Keywords: Nonlinear stretching sheet, melting heat transfer, thermal radiation, chemical reaction, slip flow, numerical solution.

***Corresponding Author: B.J. Gireesha:** Department of Studies and Research in Mathematics - Kuvempu University Shankaraghatta 577 451 , Shimoga, Karnataka 577451 India, E-mail: bjgireesu@gmail.com
M.R. Krishnamurthy: Department of Studies and Research in Mathematics, Kuvempu University, Shankaraghatta-577 451, Shimoga, Karnataka, India, E-mail: kittysa.mr@gmail.com
B.C. Prasannakumara: Government First Grade College, Koppa, Chikkamagaluru-577126, Karnataka, India, E-mail: dr.bcprasanna@gmail.com
Rama Subba Reddy Gorla: Department of Mechanical Engineering, Akron University, Akron, Ohio, USA, E-mail: rama.gorla@yahoo.com

1 Introduction

Heat, mass and momentum transfer in the laminar boundary layer flow over a stretching sheet is relevant to several industrial and engineering processes in the field of metallurgy and chemical engineering processes. These applications involve the cooling of continuous strips or filaments by drawing them through a quiescent fluid. Flow past a stretching surface with different stretching velocity, namely linear [1], exponential [2], non-linear [3], quadratic [4], hyperbolic [5], radially [6] and even oscillatory [7] has also been addressed previously. However studies on heat and mass transfer in the laminar boundary layer flow over a non- linear stretching sheet is very less. It is well known to the all research community that the stretching is not necessarily linear in many industrial applications. The problem of non-linear stretching sheet for different cases of fluid flow has also been analyzed by different researchers. Rana and Bhargava [8] numerically investigated the steady, laminar boundary fluid flow which results from the non-linear stretching of a flat surface in a nanofluid. Mondal et al. [9] carried out an analysis to study the mixed convective heat and mass transfer of nanofluids over a non-linear stretching sheet under the influence of suction/injection parameter, magnetic parameter and thermophoresis parameter. Mustafa et al. [10] obtained the analytical and numerical solutions for axisymmetric flow of nanofluid due to a nonlinearly stretching sheet. Effects of nanoparticle migration and asymmetric heating on forced convective heat transfer of alumina/water nanofluid in microchannels in presence of a uniform magnetic field was theoretically presented by Malvandi and Ganji [11]. Khan et al. [12] studied the three-dimensional flow of nanofluid over an elastic sheet stretched non-linearly in two lateral directions and the results of their study reveal that penetration depths of temperature and nanoparticle volume fraction are decreasing functions of the power-law index. Dhanai et al. [13] numerically investigated the problem of magneto-hydrodynamic

boundary layer flow of nanofluid induced by a power-law stretching/shrinking permeable sheet using shooting method, by taking the effect of viscous dissipation. Mabood et al. [14] obtained numerical results for MHD laminar boundary layer flow with heat and mass transfer of an electrically conducting water-based nanofluid over a nonlinear stretching sheet with viscous dissipation effect. Recently, Malvandi et al. [15] numerically investigated the thermal performance of hydromagnetic alumina/water nanofluid inside a vertical microannular tube by considering the different modes of nanoparticle migration. Malvandi [16] examined the anisotropic behavior of thermal conductivity and its effects on flow field and heat transfer characteristics at film boiling of MNFs over a vertical cylinder in the presence of a uniform variable-directional magnetic field.

Applying no-slip boundary condition, many authors have obtained both numerical and analytical solutions to heat, mass, and momentum transfer in the laminar boundary layer flow over a stretching surface. No-slip condition is inadequate for most non-Newtonian liquids, as some polymer melt often shows microscopic wall slip and that has a controlling influence by a nonlinear and monotone relation between the slip velocity and the traction. Partial velocity slip may occur on the stretching boundary when the fluid is particulate such as emulsions, suspensions, foams and polymer solutions. In various industrial processes, slip effects can arise at the boundary of pipes, walls, curved surfaces etc. A usual approach in studying slip phenomena is the Navier velocity slip condition. Boundary layer slip flow problems arises in polishing of artificial heart valves and internal cavities. Recently many authors obtained analytical and numerical solutions for boundary layer flow and heat transfer due to a stretching sheet with slip boundary conditions. Ibrahim and Shanker [17] commented on MHD boundary layer flow and heat transfer of a nanofluid past a permeable stretching sheet with velocity, thermal and solutal slip boundary conditions. Malvandi and Ganji [18] theoretically investigated the laminar flow and convective heat transfer of alumina/water nanofluid inside a circular microchannel in the presence of a uniform magnetic field. Nadeem et al. [19] analyzed combined effects of magnetic field and partial slip on obliquely striking rheological fluid over a stretching convective surface. Das [20] performed a numerical investigation, to study the problem of boundary layer flow of a nanofluid over non-linear permeable stretching sheet at prescribed surface temperature in the presence of partial slip. The effects of velocity slip, thermal slip and magnetic field on MHD boundary layer mixed convection flow and heat transfer of an incompressible viscous fluid over a vertical plate of very small thickness and much larger breadth in the presence of suction/blowing are presented by Mukhopadhyay and Mondal [21]. The investigation on developing the transport phenomenon of the nanofluids falling condensate film, taking into account the effects of nanoparticle migration has been presented by Malvandi et al. [22].

In the context of space technology and in the processes involving high temperatures, the effect of radiation plays a vital role. Yazdi et al. [22] presented numerical solution for MHD liquid flow and heat transfer over a non-linear permeable stretching surface in the presence of chemical reactions and partial slip. Pal and Talukdar [24] analyzed the combined effect of mixed convection with thermal radiation and chemical reaction on MHD flow of viscous and electrically conducting fluid past a vertical permeable surface embedded in a porous medium. Hady et al. [25] studied the flow and heat transfer characteristics of a viscous nanofluid over a nonlinearly stretching sheet in the presence of thermal radiation which is included in the energy equation, and variable wall temperature. Pal and Mandal [26] obtained the numerical solution by fifth-order Runge–Kutta–Fehlberg method with shooting technique for magnetohydrodynamic boundary layer flow of an electrically conducting convective nanofluids induced by a non-linear vertical stretching/shrinking sheet with viscous dissipation, thermal radiation and Ohmic heating.

Over the last few years a considerable amount of experimental and theoretical research has been carried out to determine the role of natural convection in the kinetics of heat transfer accompanied with melting or solidification effect. Processes involving melting heat transfer in non-Newtonian fluids have promising applications in thermal engineering such as oil extraction, magma solidification, melting of permafrost, geothermal energy recovery, thermal insulation, etc. Roberts [27] was the first to describe the melting phenomena of ice placed in a hot stream of air at a steady state. Epstein and Cho [28] studied melting heat transfer in steady laminar flow over a flat plate. Krishnamurthy et al. [29] presented the numerical results to study the effect of chemical reaction on MHD boundary layer flow and melting heat transfer of Williamson nanofluid in porous medium.

Based on the aforementioned literature survey, we intended to perform a theoretical investigation of MHD velocity slip boundary layer flow and melting heat transfer of nanofluids induced by a nonlinear stretching sheet under the influence of thermal radiation and chemical reaction. The Brownian motion and thermophoresis effects are considered in the present flow analysis. Reduced governing nonlinear ordinary differential equations are solved

numerically by means of Runge-Kutta-Fehlberg-45 order method. The effects of different flow parameters on flow fields are elucidated through graphs and tables.

2 Mathematical Formulation

Consider a steady two dimensional flow of water-based nanofluid induced by a nonlinear stretching surface. The sheet is extended with velocity $u_w(x) = ax^n$ with fixed origin location, where n is a nonlinear stretching parameter, a is a constant and x is the coordinate measured along the stretching surface. The flow is along x-axis and y is normal to it as shown in the Fig. 1 . A magnetic field of strength $B(x)$ is applied normal to the stretching sheet.

The wall temperature T_w and the nanoparticle fraction C_w are assumed as constant at the stretching surface. When y tends to infinity, the ambient values of temperature and nanoparticle fraction are denoted by T_∞ and C_∞, respectively. Further, let the temperature of the melting surface as T_m and temperature in the free-stream condition as T_∞, where $T_\infty > T_m$. The considered physical system is of importance in modern nano-technological fabrication and thermal materials processing. It is important to note that the constant temperature and nanoparticle fraction for the stretching surface T_m and C_w are assumed to be greater than the ambient temperature and nanoparticle fraction T_∞, C_∞, respectively.

The governing equations of momentum, thermal energy and concentration can be written as, Khan and Pop [30],

$$\frac{\partial u}{\partial x} + \frac{\partial v}{\partial y} = 0, \tag{1}$$

$$u\frac{\partial u}{\partial x} + v\frac{\partial u}{\partial y} = \nu\frac{\partial^2 u}{\partial y^2} - \frac{\sigma B^2(x)}{\rho_f}u, \tag{2}$$

$$u\frac{\partial T}{\partial x} + v\frac{\partial T}{\partial y} = \alpha\frac{\partial^2 T}{\partial y^2} + \tau\left[D_B\frac{\partial C}{\partial y}\frac{\partial T}{\partial y} + \frac{D_T}{T_\infty}\left(\frac{\partial T}{\partial y}\right)^2\right] + \frac{\nu_f}{c_f}\left(\frac{\partial u}{\partial y}\right)^2 - \frac{1}{(\rho c)_f}\frac{\partial q_r}{\partial y}, \tag{3}$$

$$u\frac{\partial C}{\partial x} + v\frac{\partial C}{\partial y} = D_B\frac{\partial^2 C}{\partial y^2} + \frac{D_T}{T_\infty}\frac{\partial^2 T}{\partial y^2} - k_0(C - C_\infty). \tag{4}$$

We assume that the variable magnetic field $B(x)$ and is of the form $B(x) = B_0 x^{\frac{n-1}{2}}$ [30–33].

The boundary conditions for velocity, temperature and nanoparticle fraction are considered as [8]:

$$y = 0: \quad u = u_w + K_1\frac{\partial u}{\partial y} \quad v = 0, \quad T = T_m, \quad C = C_w,$$

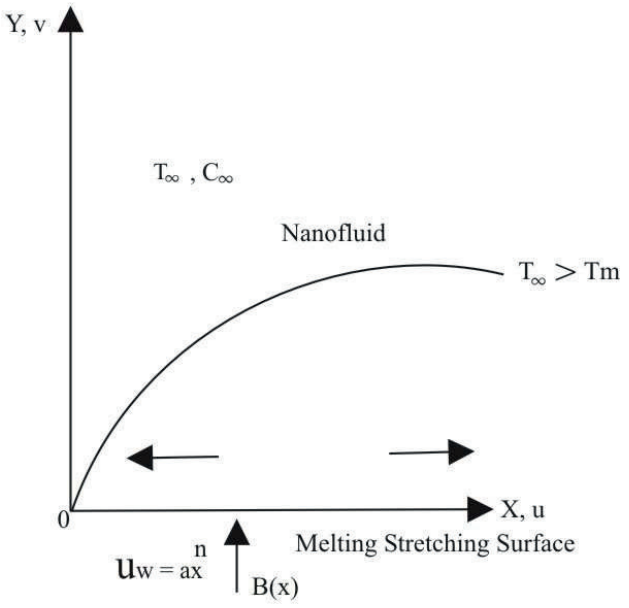

Fig. 1: Schematic representation of the flow diagram.

$$y \to \infty: \quad u \to 0, \quad T \to T_\infty, \quad C \to C_\infty. \tag{5}$$

$$k\left(\frac{\partial T}{\partial y}\right)_{y=0} = \rho_f\left[\beta + c_s(T_m - T_0)\right]v(x, 0). \tag{6}$$

$K_1 = A\sqrt{\frac{2\nu_f x}{u_w(x)(n+1)}}$ is the velocity slip factor and A is the dimensionless velocity slip parameter. Using Rosseland approximation for radiation, the radiative heat flux is simplified as,

$$q_r = -\frac{4\sigma^*}{3k^*}\frac{\partial T^4}{\partial y} \quad , \tag{7}$$

where σ^* is Stefan-Boltzmann constant and k^* the mean absorption coefficient. The temperature differences within the flow are assumed to be enough small so that T^4 may be expressed as a linear function of temperature T using a truncated Taylor series about the free stream temperature T_∞ and neglecting the higher order terms, we get,

$$T^4 \approx 4TT_\infty^3 - 3T_\infty^3 \tag{8}$$

Substituting (7) and (8) in (3), we have

$$u\frac{\partial T}{\partial x} + v\frac{\partial T}{\partial y} = \alpha\frac{\partial^2 T}{\partial y^2} + \tau\left[D_B\frac{\partial C}{\partial y}\frac{\partial T}{\partial y} + \frac{D_T}{T_\infty}\left(\frac{\partial T}{\partial y}\right)^2\right] + \frac{16\sigma^* T_\infty^3}{3k^*(\rho c)_f}\frac{\partial^2 T}{\partial y^2} + \frac{\nu_f}{c_f}\left(\frac{\partial u}{\partial y}\right)^2. \tag{9}$$

Rana and Bhargava [8] introduced the following transformations so that equation (1) is satisfied identically.

$$\eta = y\sqrt{\frac{a(n+1)}{2\nu_f}}x^{\frac{n-1}{2}}, \quad u = ax^n f'(\eta),$$
$$v = -\sqrt{\frac{a\nu_f(n+1)}{2}}x^{\frac{n-1}{2}}\left(f(\eta) + \frac{n-1}{n+1}\eta f'(\eta)\right),$$

$$\theta(\eta) = \frac{T - T_m}{T_\infty - T_m}, \quad \phi(\eta) = \frac{C - C_w}{C_\infty - C_w} \tag{10}$$

The governing equations (2), (4) and (9) are reduced into the following set of equations with the aid of equation (10) as follows:

$$f''' + ff'' - \left(\frac{2n}{n+1}\right)f'^2 - Hf' = 0, \tag{11}$$

$$\left(1 + \frac{4}{3}Nr\right)\frac{1}{Pr}\theta'' + f\theta' + Nb\theta'\phi' + Nt\theta'^2 + Ecf''^2 = 0, \tag{12}$$

$$\phi'' + Lef\phi' + \frac{Nt}{Nb}\theta'' - y\phi = 0. \tag{13}$$

The transformed boundary conditions are

$$Prf(0) + M\theta'(0) = 0, \quad f'(0) = 1 + Af''(0),$$
$$\theta(0) = 0, \quad \phi(0) = 0 \text{ at } \eta = 0,$$
$$f'(\eta) \to 0, \quad \theta(\eta) \to 1, \quad \phi(\eta) \to 1 \text{ as } \eta \to \infty, \tag{14}$$

where primes denote differentiation with respect to η, A is the velocity slip parameter and the involved physical parameters are defined as:

$$Pr = \frac{\nu_f}{\alpha} \quad Le = \frac{\nu_f}{D_B}, \quad Nb = \frac{(\rho c)_p D_B(C_\infty - C_w)}{(\rho c)_f \nu_f},$$
$$Nt = \frac{(\rho c)_p D_T(T_\infty - T_m)}{(\rho c)_f T_\infty \nu_f}, \quad H = \frac{2\sigma B_0^2}{a\rho_f(n+1)}$$
$$Ec = \frac{u_w^2}{c_f(T_\infty - T_m)}, \quad Nr = \frac{4\sigma^* T_\infty^3}{kk^*}, \quad y = \frac{k_0 Le}{a}$$
$$\text{and } M = \frac{c_f(T_\infty - T_m)}{\beta + c_s(T_m - T_0)}, \tag{15}$$

which is a combination of the Stefan number $\frac{c_f(T_\infty - T_m)}{\lambda}$ and $\frac{c_s(T_m - T_0)}{\lambda}$ for the liquid and solid phases, respectively. Here, Pr, Le, Nb, Nt, H, Ec, Nr, y and M denote the Prandtl number, the Lewis number, the Brownian motion parameter, the thermophoresis parameter, magnetic parameter, Eckert number, Radiation parameter, chemical reaction parameter and melting parameter, respectively. This boundary value problem reduces to a classical flow problem of heat and mass transfer due to a stretching surface in a viscous fluid when $n = 1$ and $Nb = Nt = 0$ in equations (12) and (13).

The quantities of practical interest, in this study, are the local skin friction coefficient C_{fx}, Nusselt number Nu_x and the Sherwood number Sh_x and are defined as,

$$C_{fx} = \frac{\mu_f}{\rho_f u_w^2}\left(\frac{\partial u}{\partial y}\right)_{y=0}, \; Nu_x = \frac{xq_w}{k(T_\infty - T_m)},$$
$$Sh_x = \frac{xq_m}{D_B(C_\infty - C_w)}, \tag{16}$$

where k is the thermal conductivity of the nanofluid, and q_w, q_m are the heat and mass fluxes at the surface, respectively and are given by

$$q_w = -k\left(\frac{\partial T}{\partial y}\right)_{y=0}, \quad q_m = -D_B\left(\frac{\partial C}{\partial y}\right)_{y=0}. \tag{17}$$

Using (10) and (17) in (16) , we obtain

$$Re_x^{-\frac{1}{2}} C_{fx} = \sqrt{\frac{n+1}{2}}f''(0),$$
$$Re_x^{-\frac{1}{2}} Nu_x = -\sqrt{\frac{n+1}{2}}\theta'(0),$$
$$Re_x^{-\frac{1}{2}} Sh_x = -\sqrt{\frac{n+1}{2}}\phi'(0), \tag{18}$$

where $Re_x = \frac{u_w x}{\nu_f}$ is the local Reynolds number.

3 Method of Solution and Validation

The system of non-linear ordinary differential equations (11)-(13) with boundary conditions (14) have been solved using Runge-Kutta-Fehlberg fourth-fifth order method along with Shooting technique. In this system of differential equations f is of third order and θ and ϕ are of second order. In the first step, f , θ and ϕ are reduced to a system of seven simultaneous differential equations of first order as follows:

$$f_1' = f_2,$$
$$f_2' = f_3,$$
$$f_3' = \left(\frac{2n}{n+1}\right)f_2^2 + Hf_2 - ff_3,$$
$$f_4' = f_5,$$
$$f_5' = \left(\frac{-Pr}{1 + 4/3Nr}\right)\left[ff_5 + Nbf_5f_7 + Ntf_5^2 + Ecf_3^2\right],$$
$$f_6' = f_7,$$
$$f_7' = yf_6 - Leff_7 - \frac{Nt}{Nb}f_5',$$

where $f_1 = f, f_2 = f', f_3 = f'', f_4 = \theta, f_5 = \theta', f_6 = \phi, f_7 = \phi'$ and prime denotes a derivative of the function with respect to η.

The corresponding boundary conditions will become

$$Prf_1 + Mf_5 = 0, \quad f_2 = 1 + Af_3 \quad f_4 = 0, \quad f_6 = 0 \text{ at } \eta = 0$$

$$f_2 = 0, \quad f_4 = 1, \quad f_6 = 1 \text{ as } \eta \to \infty.$$

The shooting technique is employed to find the values of $f_3(0)$, $f_5(0)$ and $f_7(0)$, since they are unknown. We start with some initial guess for some particular set of parameters to obtain $f_3(0)$, $f_5(0)$ and $f_7(0)$. The procedure is repeated with another value of η_∞ until two successive values of $f_3(0)$, $f_5(0)$ and $f_7(0)$ are differ only by the desired accuracy. We have compared the calculated values of $f', \theta \,\&\, \phi$ at $\eta = 10$ with the given boundary conditions and adjusting the estimated values of $f''(0), \theta'(0) \,\&\, \phi'(0)$ to give a better approximation. One has to take infinity condition at a large but finite value of η where negligible variation in velocity, temperature and so on occurs. Our bulk computations are considered with the value at $\eta_\infty =$ 8 or 10, which is sufficient to achieve the far field boundary conditions asymptotically for all values of the parameters considered.

After fixing finite value for η_∞, integration is carried out with the help of Runge-Kutta-Fehlberg-45 (RKF-45) method. This method has a procedure to determine the solution if the proper step size h is being used. At each step, two different approximations for the solution are made and compared. If the two answers are in close agreement, the approximation is accepted otherwise, the step size is reduced until to get the required accuracy. For the present problem, we took step size $\Delta\eta = 0.001$, $\eta_\infty = 8 \, or \, 10$ and accuracy to the fifth decimal places. To have a check on the accuracy of the numerical procedure used, first test computations for $\theta'(0)$ are carried out for viscous fluid for various values of Pr and compared with the available published results of Nadeem and Hussain [34], Gorla and Sidawi [35] and Goyal and Bhargava [36] in Table 1 and they are found to be in excellent agreement.

4 Results and discussion

A theoretical investigation of MHD velocity slip boundary layer flow and melting heat transfer of nanofluids over a nonlinear stretching sheet under the influence of thermal radiation and chemical reaction has been performed. The governing differential equations of the present formulation were solved numerically by means of Runge-Kutta-Fehlberg-45 order method. In order to study the behavior of velocity, temperature distribution and nanoparticle volume fraction profile for slip parameter (A), Eckert number (Ec), magnetic parameter (H), chemical reaction parameter (y), nonlinear stretching parameters (n), melting parameter (M), Radiation parameter (Nr), Brownian motion (Nb) and thermophoresis parameter (Nt), graphs are plotted and physical reasons behind the trend of the graphs are discussed.

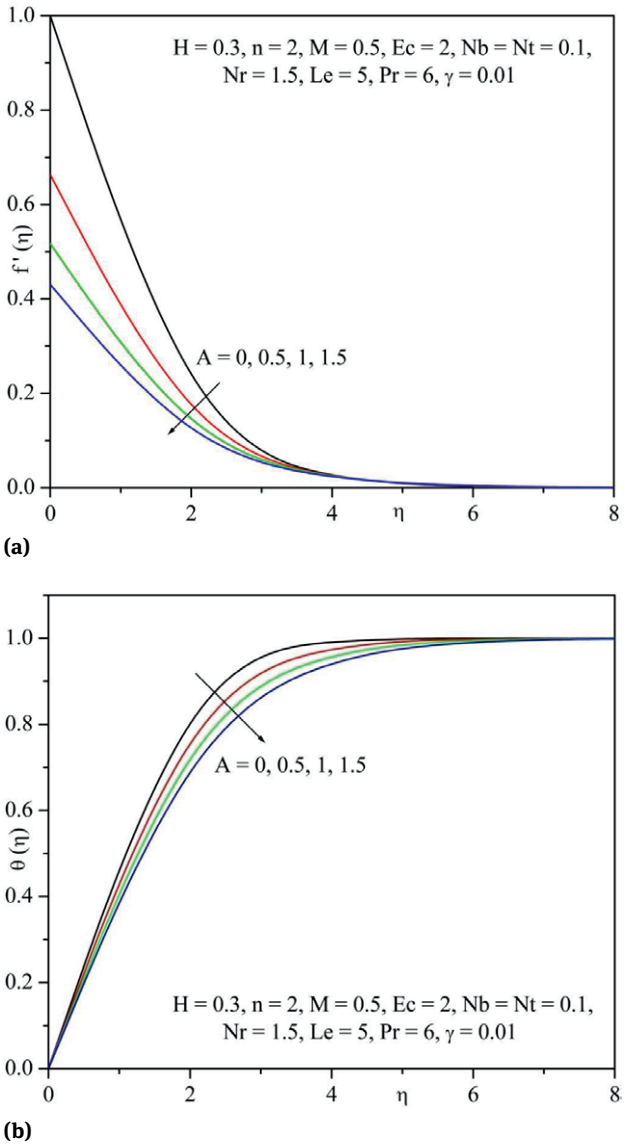

Fig. 2: (a) Effect of A on dimensionless velocity; (b) Effect of A on dimensionless temperature.

Table 1: Comparison table for $-\theta'(0)$ (viscous case) with $n = 1, H = Nr = Ec = M = 0, Nb = Nt = 10^{-6}, Le = 10$.

Pr	Nadeem and Hussain (HAM method) [34]	Gorla and Sidawi [35]	Goyal and Bhargava (FEM Method) [36]	Present (RKF45 Method)
0.2	0.169	0.1691	0.1691	0.1702
0.7	0.454	0.5349	0.4539	0.4544
2	0.911	0.9114	0.9113	0.9113
7		1.8905	1.8954	1.8954
20		3.3539	3.3539	3.3539

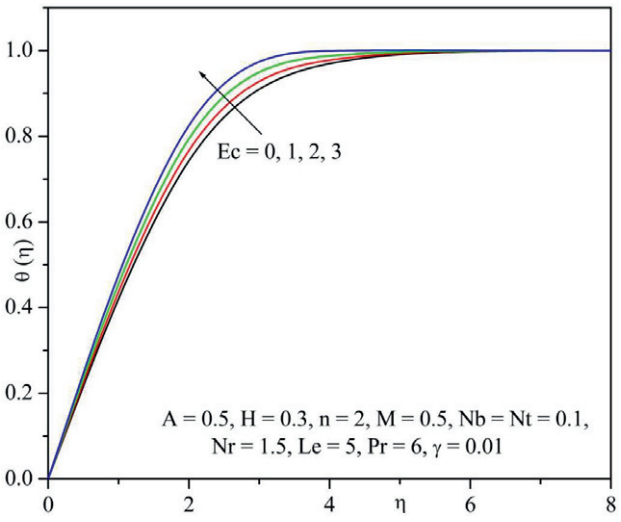

Fig. 3: Effect of Ec on dimensionless temperature.

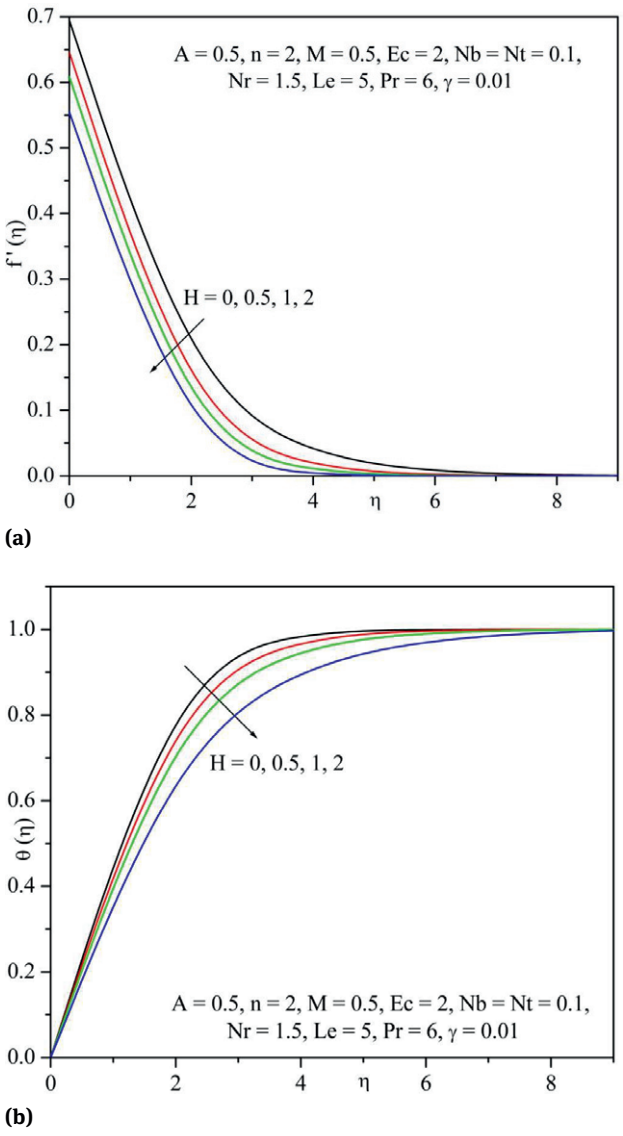

Fig. 4: Effect of H on dimensionless (a) velocity, (b) temperature.

The variations in velocity field and temperature distribution for various values of the slip parameter (A) are presented in Figs. 2(a) and 2(b). These figures shows that the effect of increasing value of A is to reducing thickness of the momentum boundary layer. Therefore, the effect of slip parameter is to decrease the boundary layer velocity while the temperature increased with increase in the slip parameter.

Fig. 3 shows the effect of dimensionless temperature profiles for Eckert number (Ec).This figure shows that the temperature profile increases for increasing values of Ec. Figs. 4(a) and 4(b) depicts the effect of magnetic parameter (H) on dimensionless velocity and temperature distributions, respectively. It is clear from these Figs. that the velocity decreases, whereas the temperature increases with increase in the magnetic parameter. This is due to the fact that the application of transverse magnetic field in an electrically conducting fluid produces a resistive force known as Lorentz force, which slow down the motion of the fluid in the boundary layer and thus reduces the velocity. The additional work done in dragging the conducting nanofluid against the action of the magnetic field, B_o is manifested as thermal energy. Thus, the presence of magnetic field decreases the momentum boundary layer thickness and increases the thermal boundary layer thickness. The warming of the boundary layer therefore also aids in nanoparticle diffusion which causes a rise in nanoparticle volume fraction.

The effect of chemical reaction parameter (y) on nanoparticle volume fraction profile is depicted in

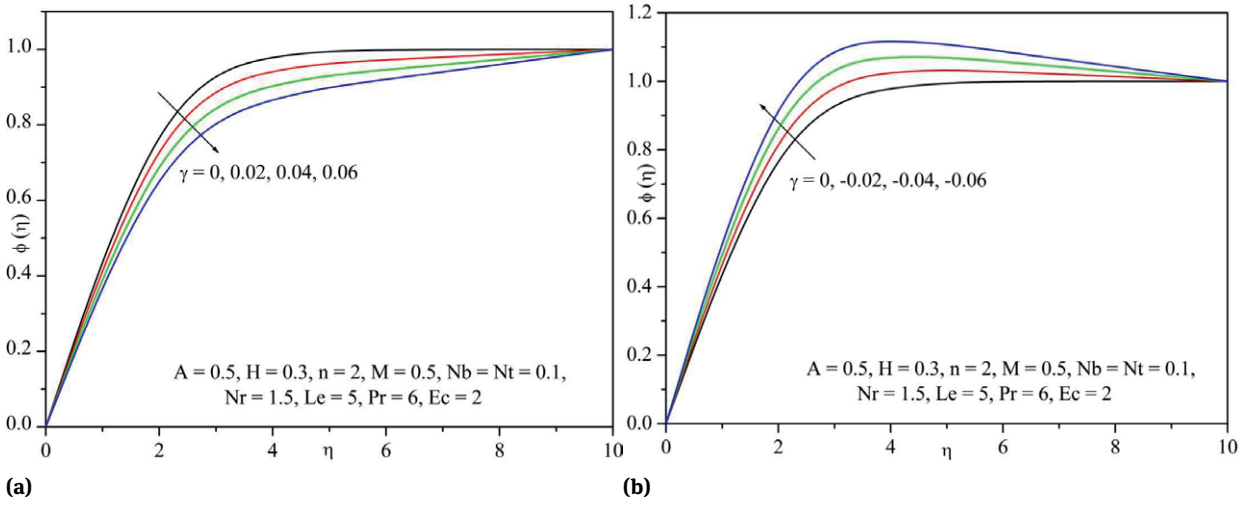

Fig. 5: (a) Effect of y on constructive dimensionless concentration. (b) Effect of y on destructive dimensionless concentration.

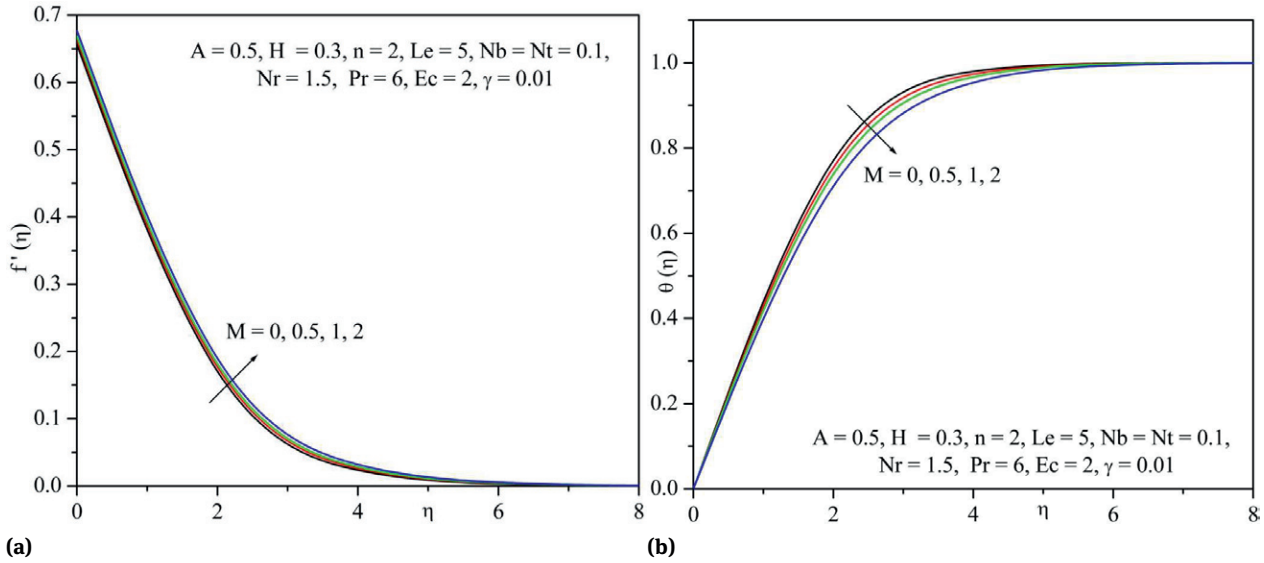

Fig. 6: Effect of M on dimensionless (a) velocity, (b) temperature.

Figs. 5(a) and 5(b) for species consumption and generation cases. It is observed that the nanoparticles volume fraction decreases for constructive chemical reaction parameter and increases for destructive chemical reaction parameter on melting surface.

Figs. 6(a) and 6(b) reveals that velocity and temperature distributions for different values of melting parameter (M). It is observed that for increasing values of M, the velocity and the boundary layer thickness increases and decreases the temperature distribution. This is because, an increase in M will increase the intensity of melting which act as blowing boundary condition at the stretching surface and hence tends to thicken the boundary layer.

Figs. 7(a) and 7(b) exhibits the effect of nonlinear stretching parameters (n) on the dimensionless velocity and temperature distributions. It is observed that the velocity profile of the nanofluid is insignificantly reduces and temperature profile increases with increasing values of n. The effect of Lewis number (Le) on temperature and concentration profiles are illustrated as in Figs. 8(a) and 8(b). It is clearly observed that the temperature profiles decreases and the nanoparticles volume fraction as well as its boundary-layer thickness increases consider-

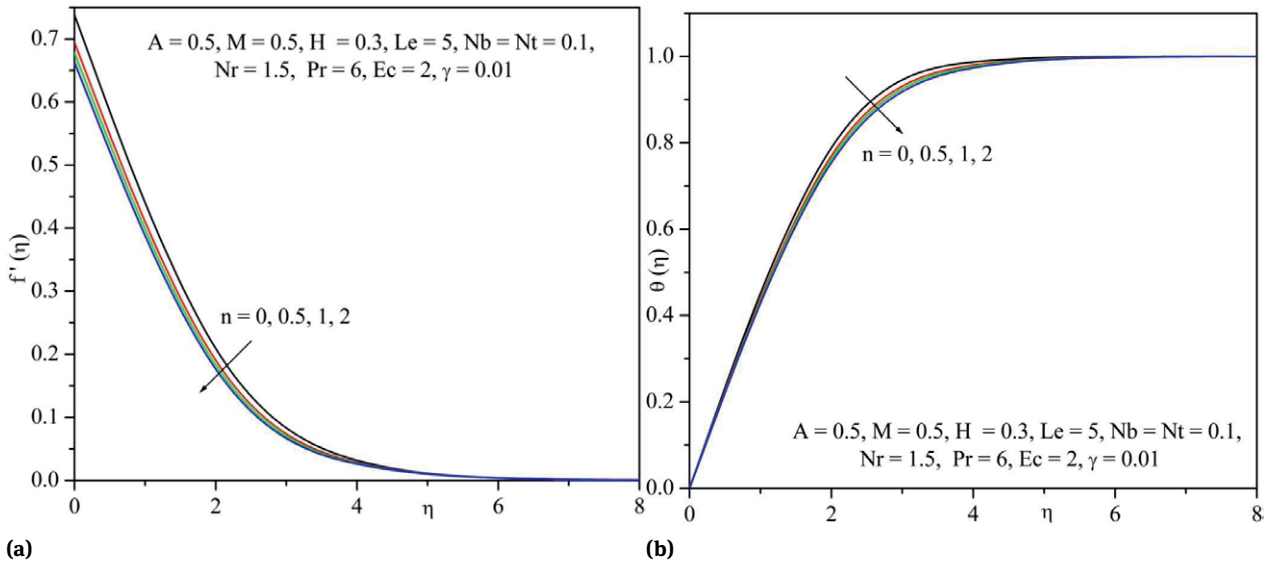

Fig. 7: Effect of n on dimensionless (a) velocity, (b) temperature.

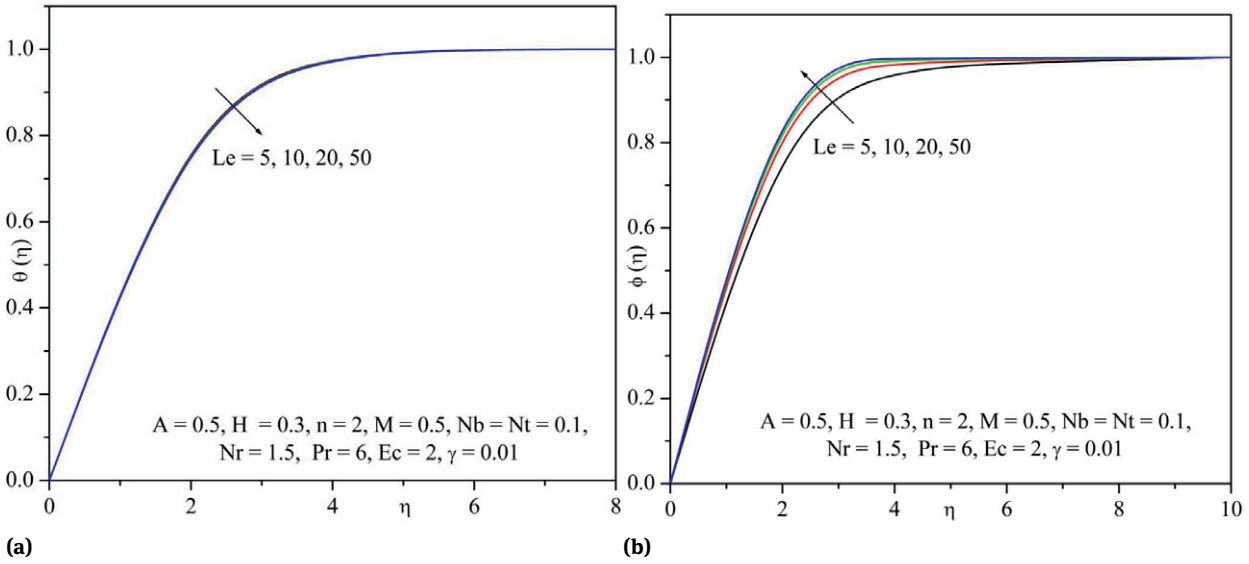

Fig. 8: Effect of Le on dimensionless (a) temperature, (b) concentration.

ably as Le increases. Physically, Le expresses the relative contribution of thermal diffusion rate to species diffusion rate in the boundary layer regime. An increase in Le values will reduce thermal boundary layer thickness and will be accompanied with a decrease in temperature and mass transfer rate increases as Le increases. It also reveals that the concentration gradient at surface of the plate increases.

Fig. 9 explains the effect of radiation parameter (Nr) on temperature profiles. It is observed that, the temperature profile decreases for increasing values of Nr. This is because, an increase in the radiation parameter Nr leads to decrease in the boundary layer thickness and enhance the heat transfer rate on melting surface in the presence of constructive chemical reaction parameter. The radiation parameter Nr being the reciprocal of the Stark number (also known as Stephan number) is the measure of relative importance of the thermal radiation transfer to the conduction heat transfer. Thus larger values of Nr show a dominance of the thermal radiation over conduction. Consequently larger values of Nr are indicative of larger amount of radiative heat energy being poured into the sys-

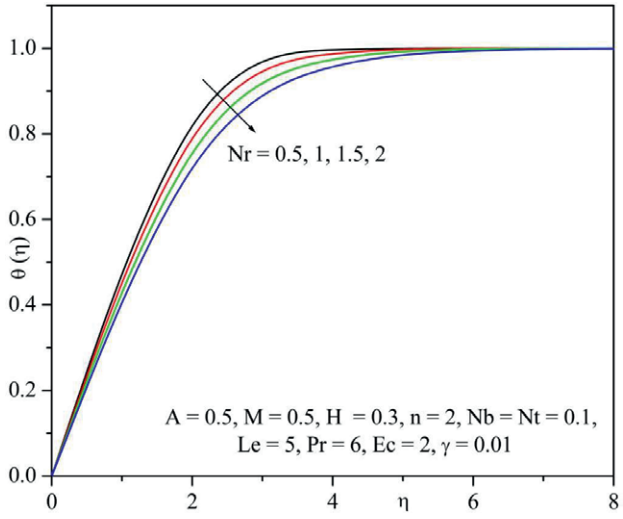

Fig. 9: Effect of *Nr* on dimensionless temperature.

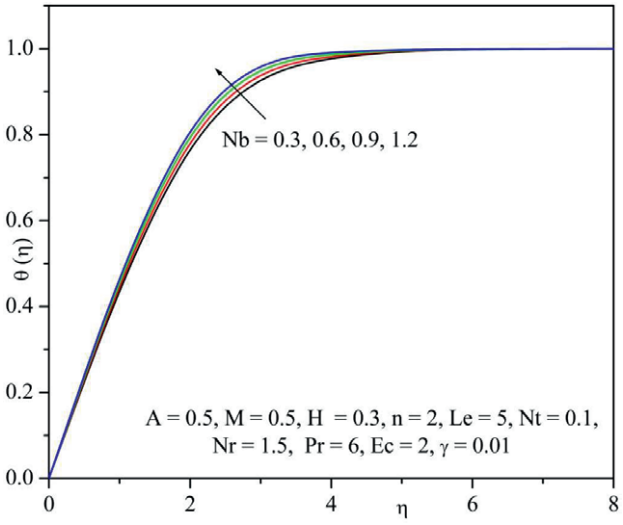

(a)

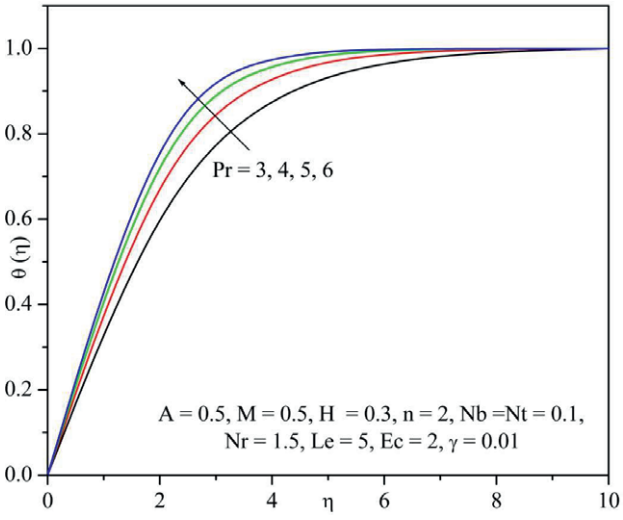

Fig. 10: Effect of *Pr* on dimensionless temperature.

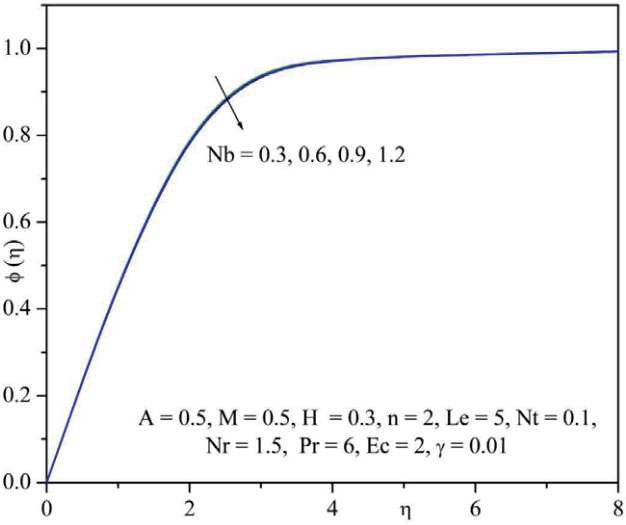

(b)

Fig. 11: Effect of *Nb* on dimensionless (a) temperature, (b) concentration.

tem, causing a rise in $\theta(\eta)$. Fig. 10 depicts the effect of Prandtl number (Pr) on temperature profiles. In the presence of melting parameter, an increase in Pr, increases the temperature profiles. Physically, larger Prandtl number possess weaker thermal diffusivity and smaller Prandtl number have stronger thermal diffusivity. This change in thermal diffusivity creates a reduction in the temperature and thermal boundary layer thickness.

The effects of Brownian motion (Nb) and thermophoresis parameter (Nt) on temperature and concentration profiles are depicted in Figs. 11(a) and 11(b), 12(a) and 12(b) respectively. From these plots, it is observed that the effect of increasing the values of Nb increases temperature profiles and decrease the concentration profiles whereas increasing values of Nt increases both the profiles.

Fig. 13 shows the effect of magnetic parameter (H) with velocity slip parameter (A) in the presence and absence of melting effect and nonlinear stretching parameter on skin friction coefficient. From this figure, it is observed that the skin friction coefficient increases for increasing values of magnetic parameter, while it decreases with velocity slip parameter. This tendency is observed in the presence and absence of melting parameter and nonlinear stretching parameter.

The effect of Brownian motion (Nb) with thermophoresis parameter(Nt) in the presence and absence of

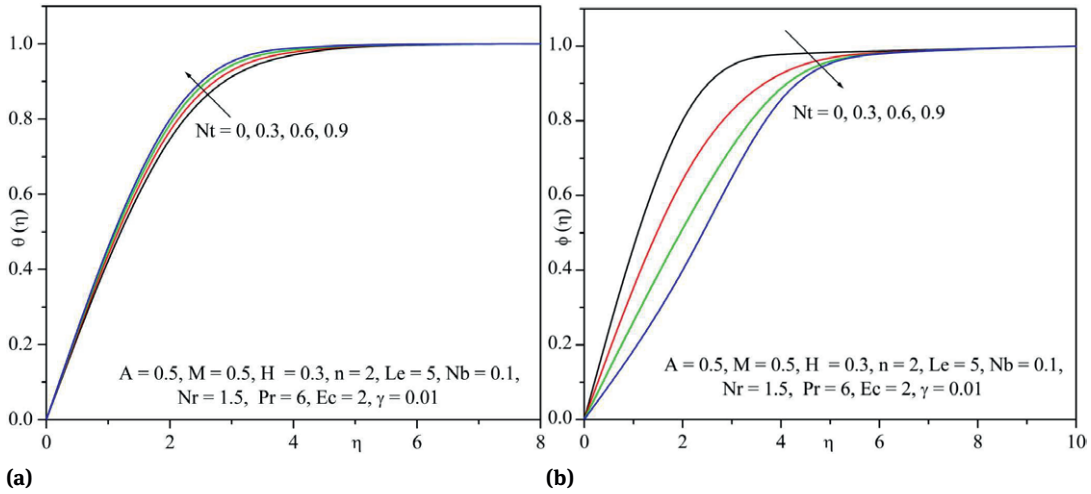

Fig. 12: Effect of *Nt* on dimensionless (a) temperature, (b) concentration.

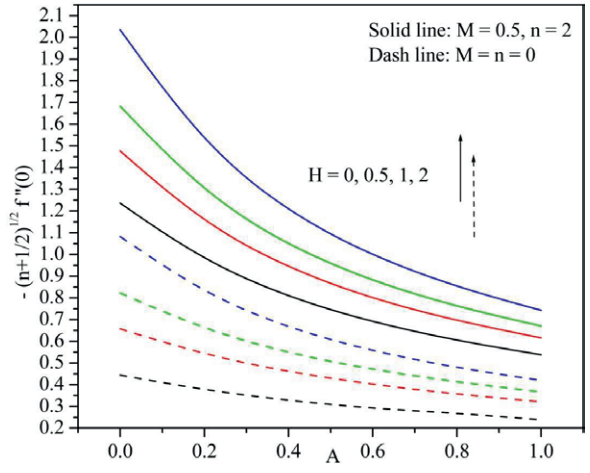

Fig. 13: Effect of *H* and *A* on skin friction coefficient.

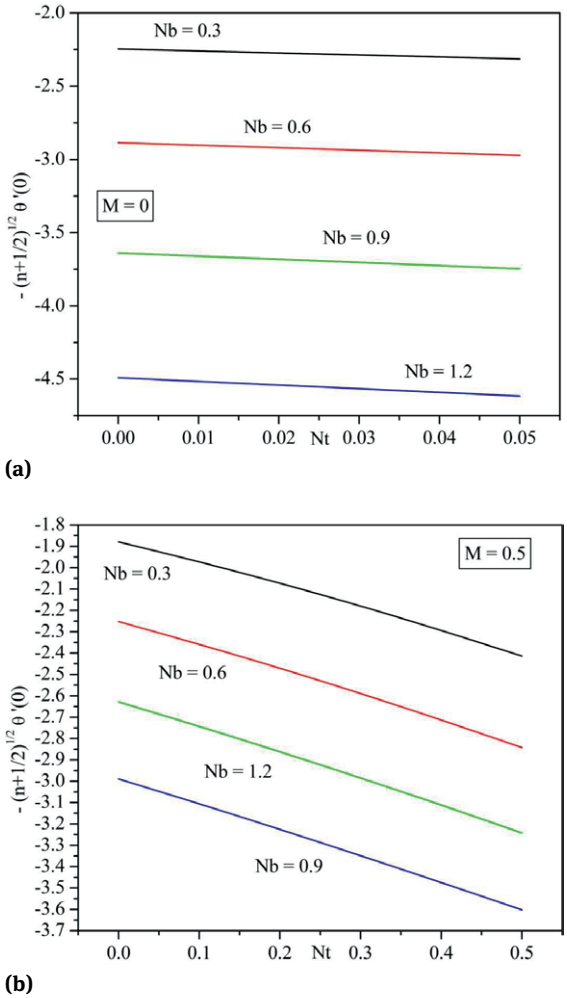

Fig. 14: Variation of heat transfer rate with *Nb* and *Nt* when (a) $M = 0$, (b) $M = 0.5$.

melting parameter on Nusselt number is illustrated respectively in the Figs. 14(a) and 14(b). From these Figs. we observed that the Nusselt number decreases with *Nt* and *Nb* on both melting and non-melting surfaces. Further, we can observe that the variations in Nusselt number is more in the presence of melting parameter when compared to its absence.

Figs. 15 and 16 shows the effect Eckert number (*Ec*) and radiation parameter (*Nr*) with Prandtl number (*Pr*) on heat transfer rate. From these Figs. we observed that the Nusselt number decreases for increasing values of *Ec* and increases for increasing values of *Nr* with *Pr* when $M = 0.5$, $n = 2$ and $M = n = 0$.

The effect of chemical reaction parameter (y) with Lewis number (Le) in the presence and absence of melting and nonlinear stretching parameter on Sherwood num-

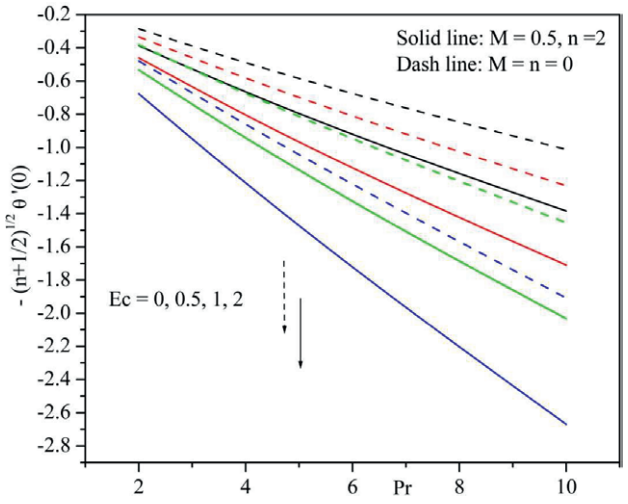

Fig. 15: Variation of heat transfer rate with Ec and Pr.

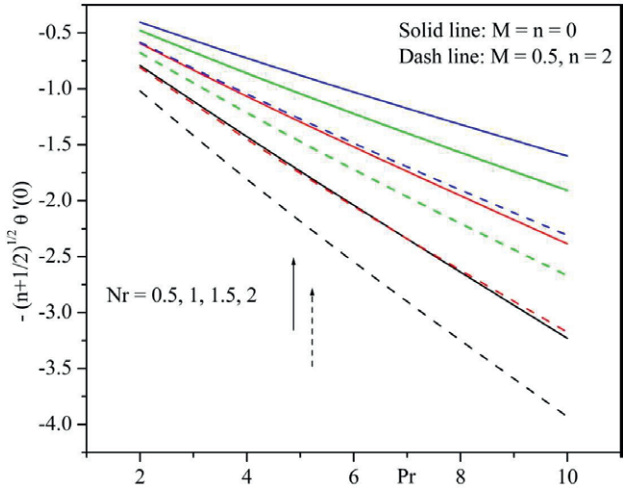

Fig. 16: Variation of heat transfer rate with Nr and Pr.

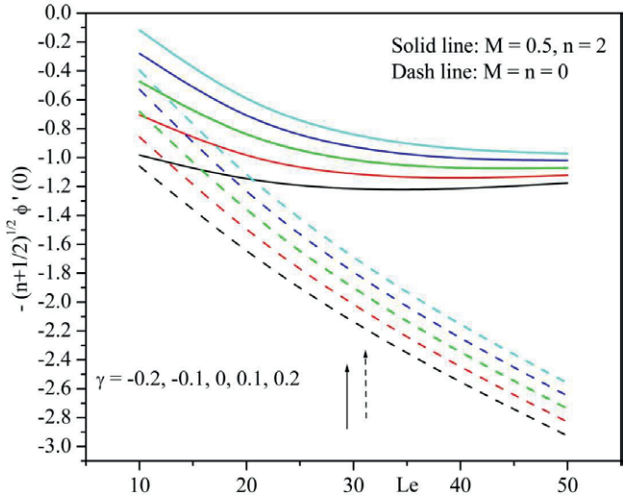

Fig. 17: Variation of concentration gradient with y and Le.

ber is shown in the Fig. 17. From these figures it is observed that the concentration gradient increases when $M = 0.5$, $n = 2$ and $M = n = 0$ for increasing values of y.

5 Conclusion

MHD boundary layer slip flow and melting heat transfer of a water-based nanofluid induced by a nonlinear stretching sheet with thermal radiation, chemical reaction and viscous dissipation has been investigated numerically. The effects of governing parameters on the flow, concentration and melting heat transfer characteristics are presented through graphs and tables. The main observations of the present study are as follows:

- The velocity decreases and the temperature will increase for velocity slip parameter.
- For increasing values of melting parameter, the velocity increases and temperature decreases.
- An increase in Brownian motion parameter and thermophoresis parameter is to increase the temperature in the thermal boundary layer which consequently reduces the heat transfer rate at the surface when both $M = 0$ and $M = 0.5$.
- Both in the presence and absence of nonlinear stretching parameter and melting parameter, the skin friction coefficient increases, where as the reduced Nusselt numbers decrease for increasing values of magnetic parameter and velocity slip parameter.
- The Nusselt number decreases for Eckert number and increases for radiation parameter when $M = 0.5$, $n = 2$ and $M = n = 0$.

6 Nomenclature

a	stretching rate of the sheet (s^{-1})
A	dimensionless velocity slip parameter
$B(x)$	magnetic field of strtength
B_0	induced magnetic field
C	rescaled nanoparticle volume fraction
c_f	specific heat coefficient of fluid ($J/kg\,K$)
C_{fx}	skin friction coefficient
c_p	specific heat coefficient of nanoparticles ($J/kg\,K$)
c_s	heat capacity of the solid surface
C_w	concentration at the wall (kg/m^3)

C_∞	ambient nanofluid volume fraction (kg/m^3)
D_B	Brownian diffusion coefficient
D_T	thermophoresis diffusion coefficient
Ec	Eckert number
H	magnetic parameter
k	thermal conductivity (W/mK)
k_0	chemical reaction coefficient
K_1	velocity slip factor
k^*	mean absorption coefficient (W/mK)
Le	Lewis number
M	melting parameter
n	nonlinear stretching parameter
Nb	Brownian motion parameter
Nt	thermophoresis parameter
Nr	radiation parameter
Nu_x	Nusselt number
Pr	Prandtl number
q_r	radiative heat flux (Wm^{-2})
q_w	surface heat flux
Re_x	local Reynolds number
Sh_x	Sherwood number
T	fluid temperature (K)
T_0	solid surface temperature (K)
T_w	uniform wall temperature
T_m	temperature of the melting surface
T_∞	ambient Surface temperature (K)
$(u,\ v)$	velocity components along the x and y axis (ms^{-1})
$u_w(x)$	stretching velocity
xy	coordinates (m)
	Greek Symbols
$\alpha = \frac{k}{(\rho c)_f}$	thermal diffusivity $(m^2\ s^{-1})$
β	latent heat of the fluid
η	dimensionless similarity variable
y	chemical reaction parameter
ν_f	kinematic viscosity $(m^2 s^{-1})$
ϕ	dimensionless nanoparticle volume fraction
ρ_f	density of the base fluid (kgm^3)
ρ_p	density of the nanoparticles (kgm^3)
σ	electrical conductivity
σ^*	Stefan-Boltzmann constant $(Wm^{-2}\ K^{-4})$
θ	dimensionless temperature variable
$\tau = \frac{(\rho c)_p}{(\rho c)_f}$	ratio between the effective heat capacity of the nanoparticle material and heat capacity of the fluid
τ_w	surface shear stress
	Subscripts
∞	infinity
w	sheet surface

Acknowledgement: One of the author B.C.Prasannakumara is thankful to the University Grants Commission, India, for the financial support under the Major research project Scheme[F.No.43-419/2014(SR)].

References

[1] G. K. Ramesh and B. J. Gireesha, "Influence of heat source/sink on a Maxwell fluid over a stretching surface with convective boundary condition in the presence of nanoparticles", Ain Shams Eng. J., 5(3) (2014) 991–998.

[2] T. Hayat, M. Imtiaz, A. Alsaedi and R. Mansoor, "MHD flow of nanofluids over an exponentially stretching sheet in a porous medium with convective boundary conditions", Chin. Phys. B., 23(5) (2014) 054701.

[3] M. Mustafa and J. A. Khan, "Model for flow of Casson nanofluid past a non-linearly stretching sheet considering magnetic field effects", AIP Advances, 5, (2015) 077148.

[4] S. Kumar Khan, E. Sanjayanand, "Viscoelastic boundary layer MHD flow through a porous medium over a porous quadratic stretching sheet", Arch. Mech., 56(3) (2004) 191–204.

[5] A. Ahmad and S. Asghar, "Flow and heat transfer over hyperbolic stretching sheets", Appl. Math. Mech., 33(4) (2012) 445-454.

[6] M. Khan, A. Munir, A. Shahzad and A. Shah, "MHD flow and heat transfer of a viscous fluid over a radially stretching power-law sheet with suction/injection in a porous medium", J. App. Mech.Techn. Phy., 56(2) (2015) 231–240.

[7] S.U. Khan, N. Ali and Z. Abbas, "Hydromagnetic flow and heat transfer over a porous oscillating stretching surface in a viscoelastic fluid with porous medium", PLoS ONE, 10(12) (2015) e0144299.

[8] P. Rana and R. Bhargava, "Flow and heat transfer of a nanofluid over a nonlinearly stretching sheet: a numerical study", Commun. Nonlinear Sci. Numer. Simulat., 17 (2012) 212–226.

[9] H. Mondal, S. Mishra and U.K. Bera, "Nanofluids on MHD mixed convective heat and mass transfer over a non-linear stretching surface with suction/injection", J. Nanofluids, 4(2) (2015) 223–229.

[10] M. Mustafa, J.A. Khan, T. Hayat and A. Alsaedi, "Analytical and numerical solutions for axisymmetric flow of nanofluid due to non-linearly stretching sheet", Int. J. Non-Linear Mech., 71 (2015) 22–29.

[11] A. Malvandi and D.D. Ganji, "Effects of nanoparticle migration and asymmetric heating on magnetohydrodynamic forced convection of alumina/water nanofluid in microchannels", European Journal of Mechanics - B/Fluids, 52 (2015) 169–184.

[12] J.A. Khan, M. Mustafa, T. Hayat and A. Alsaedi, "Three-dimensional flow of nanofluid over a non-linearly stretching sheet: An application to solar energy", Int. J. Heat and Mass Transf., 86 (2015) 158–164.

[13] R. Dhanai, P. Rana and L. Kumar, "Multiple solutions of MHD boundary layer flow and heat transfer behavior of nanofluids induced by a power-law stretching/shrinking permeable sheet with viscous dissipation", Powder Technology, 273 (2015) 62–70.

[14] F. Mabood, W.A. Khan and A. I. M. Ismail, "MHD boundary layer flow and heat transfer of nanofluids over a nonlinear stretching sheet: A numerical study", J. Magnetism and Magnetic Materials, 374 (2015) 569–576.

[15] A. Malvandi, A. Ghasemi and D.D. Ganji, "Thermal performance analysis of hydromagnetic Al_2O_3-water nanofluid flows inside a concentric microannulus considering nanoparticle

migration and asymmetric heating", International Journal of Thermal Sciences, 109 (2016) 10–22.
[16] A. Malvandi, "Anisotropic behavior of magnetic nanofluids (MNFs) at film boiling over a vertical cylinder in the presence of a uniform variable-directional magnetic field", Powder Technology, 294 (2016) 307–314.
[17] W. Ibrahim and B. Shankar, "MHD boundary layer flow and heat transfer of a nanofluid past a permeable stretching sheet with velocity, thermal and solutal slip boundary conditions", Computers & Fluids, 75 (2013) 1–10.
[18] A. Malvandi and D. D. Ganji, "Brownian motion and thermophoresis effects on slip flow of alumina/water nanofluid inside a circular microchannel in the presence of a magnetic field", International Journal of Thermal Sciences, 84 (2014) 196–206.
[19] S. Nadeem, R. Mehmood and N.S. Akbar, "Combined effects of magnetic field and partial slip on obliquely striking rheological fluid over a stretching surface", J. Magnetism and Magnetic Materials, 378 (2015) 457–462.
[20] Kalidas Das, "Nanofluid flow over a non-linear permeable stretching sheet with partial slip," J. Egyptian Math. Soc., 23 (2015) 451–456.
[21] S. Mukhopadhyay and I. C. Mandal, "Magnetohydrodynamic (MHD) mixed convection slip flow and heat transfer over a vertical porous plate", Eng. Sci. Technology, 18(1) (2015) 98–105.
[22] A. Malvandi, D.D. Ganji and I. Pop, "Laminar film wise condensation of nanofluids over a vertical plate considering nanoparticles migration", Applied Thermal Engineering, 100 (2016) 979–986.
[23] M. H. Yazdi, S. Abdullah, I. Hashim and K. Sopian, "Slip MHD liquid flow and heat transfer over non-linear permeable stretching surface with chemical reaction", Int. J. Heat and Mass Transf., 54 (2011) 3214–3225.
[24] D. Pal and B. Talukdar, "Buoyancy and chemical reaction effects on MHD mixed convection heat and mass transfer in a porous medium with thermal radiation and Ohmic heating", Commun. Nonlinear Sci. Numer. Simulat., 15 (2010) 2878–2893.
[25] F. M. Hady, F. S. Ibrahim, Sahar M. Abdel-Gaied and Mohamed R. Eid, "Radiation effect on viscous flow of a nanofluid and heat transfer over a nonlinearly stretching sheet", Nanoscale Research Letters, 7 (2012) 229.
[26] D. Pal and G. Mandal, "Hydromagnetic convective–radiative boundary layer flow of nanofluids induced by a non-linear vertical stretching/shrinking sheet with viscous–Ohmic dissipation", Powder Technology, 279 (2015) 61–74.
[27] L. Roberts, "On the Melting of a semi-infinite body of ice placed in a hot stream of air", J. Fluid Mech., 4 (1958) 505–528.
[28] M. Epstein and D.H. Cho, "Melting heat transfer in steady laminar Flow over a flat plate", J. Heat transf., 98(3) (1976) 531–533.
[29] M. R. Krishnamurthy, B. C. Prasanna Kumara, B. J. Gireesha and Rama Subba Reddy Gorla, "Effect of chemical reaction on MHD boundary layer flow and melting heat transfer of Williamson nanofluid in porous medium", Engineering Science and Technology, an International Journal, 19 (2016) 53–61.
[30] W. A. Khan and I. Pop, "Boundary layer flow of a nanofluid past a stretching sheet", Int. J. Heat Mass Transf., 53 (2010) 2477–2483.
[31] K. A. Helmy, "Solution of the boundary layer equation for a power law fluid in magneto-hydrodynamics", Acta. Mech., 102 (1994) 25–37.
[32] T. C. Chiam, "Hydromagnetic flow over a surface stretching with a power-law velocity", Int. J. Eng. Sci., 33 (1995) 429–435.
[33] A. Ishak, R. Nazar and I. Pop, "Hydromagnetic flow and heat transfer adjacent to a stretching vertical sheet", Heat Mass Transf., 44 (2008) 921–927.
[34] S. Nadeem and S.T. Hussain, "Flow and heat transfer analysis of Williamson nanofluid", Appl. Nanosci., 4(8) (2013) 1005–1012.
[35] R. S. R. Gorla and I. Sidawi, "Free convection on a vertical stretching surface with suction and blowing", Appl. Sci. Res., 52 (1994) 247–257.
[36] M. Goyal and R. Bhargava, "Boundary layer flow and heat transfer of viscoelastic nanofluids past a stretching sheet with partial slip conditions", Appl. Nanosci., 4(6) (2014) 761–767.